Available online at www.sciencedirect.com

SCIENCE DIRECT

Developmental Biology 279 (2005) 205–219

DEVELOPMENTAL BIOLOGY

www.elsevier.com/locate/ydbio

Attenuation of retinal vascular development and neovascularization during oxygen-induced ischemic retinopathy in Bcl-2−/− mice

Shoujian Wang[a], Christine M. Sorenson[b], Nader Sheibani[a,c,*]

[a]*Department of Ophthalmology and Visual Sciences, University of Wisconsin Medical School, Madison, WI 53792, USA*
[b]*Department of Pediatrics, University of Wisconsin Medical School, Madison, WI 53792, USA*
[c]*Department of Pharmacology, University of Wisconsin Medical School, Madison, WI 53792, USA*

Received for publication 1 July 2004, revised 18 November 2004, accepted 8 December 2004

Abstract

Bcl-2 is a death repressor that protects cells from apoptosis mediated by a variety of stimuli. Bcl-2 expression is regulated by both pro- and anti-angiogenic factors; thus, it may play a central role during angiogenesis. However, the role of bcl-2 in vascular development and growth of new vessels requires further delineation. In this study, we investigated the physiological role of bcl-2 in development of retinal vasculature and retinal neovascularization during oxygen-induced ischemic retinopathy (OIR). Mice deficient in bcl-2 exhibited a significant decrease in retinal vascular density compared to wild-type mice. This was attributed to a decreased number of endothelial cells and pericytes in retinas from bcl-2−/− mice. We observed, in bcl-2−/− mice, delayed development of retinal vasculature and remodeling, and a significant decrease in the number of major arteries, which branch off from near the optic nerve. Interestingly, hyaloid vessel regression, an apoptosis-dependent process, was not affected in the absence of bcl-2. The retinal vasculature of bcl-2−/− mice exhibited a similar sensitivity to hyperoxia-mediated vessel obliteration compared to wild-type mice during OIR. However, the degree of ischemia-induced retinal neovascularization was significantly reduced in bcl-2−/− mice. These results suggest that expression of bcl-2 is required for appropriate development of retinal vasculature as well as its neovascularization during OIR.

Keywords: Bcl-2; Angiogenesis; Apoptosis; Retinal vascularization; Retinopathy of prematurity; Hyaloid vasculature

Introduction

Apoptosis plays an integral role during development, remodeling, and maintenance of multicellular organisms through the removal of damaged and unwanted cells. Vascular cell apoptosis plays an important role in controlling the morphology and cellular composition of the blood vessel wall. Bcl-2 family members affect cell death in either a positive or negative fashion. The founding family member, bcl-2, inhibits apoptosis. Although some redundancy exists between family members, expression of certain family members in an organ-specific manner is important during development.

Recent studies have demonstrated that modulation of bcl-2 expression is central to the activity of pro- and anti-angiogenic factors. Angiogenic factors such as basic fibroblast growth factor (FGF2) and vascular endothelial growth factor (VEGF) mediate their effects, at least in part, through enhanced expression of bcl-2 (Gerber et al., 1998; Karsan et al., 1997; Longoni et al., 2001; Nor et al., 1999; Xin et al., 2001). In contrast, most antiangiogenic factors, including thrombospondin-1 and endostatin, inhibit angiogenesis by inducing endothelial cell apoptosis through down-regulation of bcl-2 expression (Dhanabal et al., 1999; Jimenez et al., 2000). In addition, overexpression of bcl-2 not only enhances formation of blood vessels but also

* Corresponding author. University of Wisconsin Medical School, Department of Ophthalmology and Visual Sciences, 600 Highland Avenue, K6/458 CSC, Madison, WI 53792-4673, USA. Fax: +1 608 265 6021.
E-mail address: nsheibanikar@wisc.edu (N. Sheibani).

0012-1606/$ - see front matter © 2004 Elsevier Inc. All rights reserved.
doi:10.1016/j.ydbio.2004.12.017

promotes progressive maturation of vasculature by recruitment of vascular smooth muscle cells/pericytes (Biroccio et al., 2000; Nor et al., 2001).

The mouse retinal vasculature develops postnatally and is readily amenable to manipulation and biochemical examination in whole mount preparations. This provides a unique opportunity to study all aspects of vascular development, remodeling, and pruning. In addition, development of the retinal vasculature is important in the context of retinopathies in which abnormal vessel growth in the retina can ultimately lead to blindness. Apoptosis of endothelial cells (EC) during vascular remodeling and vascular regression plays an important role during development of the vasculature and is tightly regulated by expression of pro- and anti-apoptotic factors (Pollman et al., 1999; Walsh et al., 2000; Wang et al., 2003). However, the identity of these factors and, specifically, the role bcl-2 plays during these processes require further investigation.

The bcl-2−/− mice are viable but exhibit marked lymphocyte, neuronal and intestinal apoptosis, develop renal hypoplasia/cystic dysplasia, and are hypopigmented (reviewed in Sorenson, 2004). To gain a better understanding of the physiological role bcl-2 plays in retinal vascular development and neovascularization during oxygen-induced ischemic retinopathy (OIR), we have used bcl-2−/− mice. Here we demonstrate that bcl-2−/− mice exhibit decreased retinal vascular density during development of retinal vasculature. This was mainly attributed to decreased numbers of endothelial cells and pericytes, which are more sensitive to apoptosis in the absence of bcl-2. This is consistent with increased rates of apoptosis in retinal vasculature of bcl-2−/− mice. Hyaloid vessel regression, an apoptosis-dependent process, was not affected in bcl-2−/− mice. The retinal vasculature of bcl-2−/− mice exhibited a similar sensitivity to hyperoxia-mediated vessel obliteration compared to wild-type mice during oxygen-induced ischemic retinopathy (OIR). However, retinas from bcl-2−/− mice were protected from ischemia-driven neovascularization. These studies demonstrate an important role for bcl-2 during development and remodeling of retinal vasculature and its neovascularization during OIR.

Materials and methods

Tissue preparation

The targeting of the bcl-2 gene and the generation of mutant mice have been previously described (Veis et al., 1993). Litters produced by mating heterozygote mutant mice were genotyped by PCR of genomic DNA extracted from tail biopsies. Bcl-2−/− mice and wild-type mice were maintained at the University of Wisconsin animal facilities, and studies were performed according to approved protocols. For oxygen-induced ischemic retinopathy, 7-day-old (P7) pups and mothers were placed in an airtight incubator and exposed to an atmosphere of 75 ± 0.5% oxygen for 5 days. Incubator temperature was maintained at 23 ± 2°C and oxygen was continuously monitored with a PROOX model 110 oxygen controller (Reming Bioinstruments Co., Redfield, NY). Mice were then brought to room air for 5 days, and then pups were sacrificed for retinal whole mount preparations as described below.

Trypsin-digested retinal vessel preparation

Eyes were enucleated from P21 or P42 mice, fixed in 4% paraformaldehyde for at least 24 h. The eyes were bisected equatorially and the entire retina was removed under the dissecting microscope. Retinas were washed overnight in distilled water and incubated in 3% trypsin (Trypsin 1:250, Difco) prepared in 0.1 M Tris, 0.1 M maleic acid, pH7.8 containing 0.2 M NaF for approximately 1–1.5 h at 37°C. Following completion of digestion, retinal vessels were flattened by four radial cuts and mounted on glass slides for periodic acid-schiff (PAS) and hematoxylin staining. Nuclear morphology was used to distinguish pericytes from EC. The nuclei of EC are oval or elongated and lie within the vessel wall along the axis of the capillary, while pericyte nuclei are small, spherical, stain densely, and generally have a protuberant position on the capillary wall. The stained and intact retinal whole mounts were coded, and subsequent counting was performed masked.

The number of EC and pericytes was determined by counting respective nuclei under the microscope at a magnification of 400×. A mounting reticle (10 μm × 10 μm) was placed in one of the viewing oculars to facilitate counting. Only retinal capillaries were included in the cell count, which was performed in the mid-zone of the retina. We counted the number of EC and pericytes in four reticles from the four quadrants of each retina. The total number of EC and pericytes for each retina was determined by adding the numbers from the four reticles. The ratio of EC to pericytes was then calculated. To evaluate the density of cells in the capillaries, the mean number of EC or pericytes was recorded in four reticles from the four quadrants of each retina.

Visualization of retina vasculature and quantification of avascular area

Vessel obliteration and the retinal vascular pattern were analyzed using retinal whole mounts stained with anti-PECAM-1 antibody as described previously (Wang et al., 2003). At various times, the eyes of mice were enucleated and briefly fixed in 4% paraformaldehyde (10 min on ice). The eyeballs were fixed in 70% ethanol for at least 24 h at −20°C. Retinas were dissected in PBS and then washed with PBS three times, 10 min each. Following incubation in a blocking buffer (50% fetal calf serum, 20% normal goat serum in PBS) for 2 h, the retinas were incubated with rabbit anti-mouse PECAM-1 (prepared in our laboratory and

diluted 1:250 in PBS containing 20% fetal calf serum, 20% normal goat serum) at 4°C overnight. Retinas were then washed three times with PBS, 10 min each, incubated with secondary antibody Alexa 594 goat-anti-rabbit (Molecular probes; 1:500 dilution prepared in PBS containing 20% FCS, 20% NGS) for 2 h at RT, washed four times with PBS, 30 min each, and mounted on a slide with PBS/glycerol (2 vol/1 vol). Retinas were viewed by fluorescence microscopy and images were captured in digital format using a Zeiss microscope (Carl Zeiss, Chester, VA). The central capillary dropout area was quantified, as a percentage of the whole retina area, from the digital images in masked fashion using Axiovision software (Carl Zeiss, Chester, VA).

Quantification of neovascular proliferative retinopathy

Quantification of vitreous neovascularization on P17 was performed as previously described (Wang et al., 2003). Briefly, mouse eyes were enucleated, fixed in formalin for 24 h, and embedded in paraffin. Serial sections (6 μm thick), each separated by at least 40 μm, were taken from around the region of the optic nerve. The hematoxylin- and PAS-stained sections were examined in masked fashion for the presence of neovascular tufts projecting into the vitreous from the retina. The neovascular score was defined as the mean number of neovascular nuclei per section found in eight sections (four on each side of the optic nerve) per eye.

BrdU and collagen IV staining of whole mount retinas

The detection of cellular proliferation on retinal blood vessels was assessed by immunohistochemistry for 5-bromo-2-deoxyuridine (BrdU) incorporation and type IV collagen (staining blood vessels). Mice were injected intraperitoneally with 5-bromo-2-deoxyuridine (BrdU; Sigma, St. Louis, MO) 0.12 g/kg of body mass dissolved in water. One and a half hours later, the animals were sacrificed and eyes were removed and fixed immediately in 4% paraformaldehyde for 3 min on ice. Eyes were then transferred to 70% ethanol (v/v) and stored at −20°C for 2–72 h. Retinas were dissected in PBS, washed for 30 min in PBS containing 1% Triton X-100 to permeabilize cell membranes, and placed in 2 M HCl at 37°C for 1 h. Each retina was then washed in 0.1 M sodium borate for 30 min to neutralize the HCl. Retinas were then washed in PBS containing 1% Triton X-100 for 15 min and incubated with a monoclonal antibody to BrdU (Cat No. 1170376, Roche, Indianapolis, IN; diluted 1:250 in PBS containing 1% bovine serum albumin, BSA) at 4°C overnight or at room temperature for 2 h. Following incubation, retinas were washed for 10 min in PBS containing 1% Triton X-100 and incubated with anti-mouse CY2 antibody (Jackson's Laboratory) diluted 1:500 in PBS containing 1% BSA for 2 h. Retinas were then washed in PBS and stained with anti-collagen IV (Chemicon) antibody as described for PECAM-1 staining of whole mount retinas. The collagen IV antibody and secondary antibody were used at 1:1000 and 1:500, respectively. After a final wash in PBS for 30 min, the retinas were mounted with the ganglion cell layer uppermost in PBS/glycerol (2 vol/1 vol). Retinas were viewed by fluorescence microscopy and images were captured in digital format using a Zeiss microscope (Carl Zeiss, Chester, VA). For quantification, the numbers of BrdU-positive nuclei on the blood vessels were determined per retina.

TdT-dUTP terminal nick-end labeling and Caspase-3 staining

Apoptotic cell death on the retinal vasculature was assessed by two different methods. TdT-mediated dUTP-biotin nick-end labeling (TUNEL) staining was performed on 9-μm frozen eye sections with the "MEBSTAIN Apoptosis Kit II" (Medical and Biological Laboratories, Watertown, MA) as recommended by the supplier. Briefly, the slides were preincubated with the TdT buffer II for 20 min at room temperature and subsequently incubated with TdT solution (mixture of TdT buffer, Biotin-dUTP, and TdT) for 2 h at 37°C. The reaction was terminated by incubation with blocking solution at RT for 20 min. TUNEL labeling was visualized by incubation with avidin-FITC II. TUNEL-positive cell nuclei were visualized using a fluorescence microscope and photographed in digital format as described above. As an alternative, activated caspase-3 was detected by immunohistological staining of whole mount retinas. After fixation as above, retinas were dissected in PBS and permeabilized in PBS with 1% (w/v) Triton X-100 for 45 min. The whole mount retinas were incubated overnight at 4°C with a cleaved, activated caspase-3 antibody at 1:100 dilution (rabbit polyclonal, Asp 175; Cell Signaling Technology, Beverley, MA) as described for PECAM-1 staining. Alex 594 goat anti-rabbit IgG (1:400 dilution, Molecular Probes) was used as a secondary antibody. To identify whether cells showing caspase-3 immuno-reactivity are the cells on the retinal vessels, retinal vasculature was also labeled with FITC-conjugated B4-lectin (1:100 dilution, Sigma, St. Louis, MO) and visualized as above. The retinas were examined using a 20× objective under the fluorescence microscope and the number of caspase-3-positive cells in the retinal vasculature was determined in identical quadrants from each retina. Results are expressed as the mean number of positive staining cells from each retina.

Immunohistochemical staining of the frozen sections

Mouse eyes were enucleated and embedded in optimal cutting temperature (OCT) compound at −80°C. Sections (9 μm) were cut on a cryostat, placed on glass slides, and allowed to dry for 2 h. For fluorescence microscopy,

sections were fixed in cold acetone (4°C) on ice for 10 min, followed by three washes with PBS, 5 min each. Sections were incubated in blocker (1% BSA, 0.2% skim milk, and 0.3% Triton X-100 in PBS) for 15 min at room temperature. Sections were then incubated with rabbit anti-mouse type IV collagen (Chemicon) (1:500 dilution prepared in blocking solution) overnight at 4°C in humid environment. After three washes in PBS, 5 min each, sections were incubated with secondary antibody Alexa 594 goat-anti-rabbit (Molecular Probes) (1:500 dilution prepared in blocking solution). Sections were washed three times in PBS, covered with PBS/glycerol (2 vol/1 vol), and mounted with a coverslip. Retina sections were viewed by fluorescence microscopy and images were captured in digital format using a Zeiss microscope (Carl Zeiss, Chester, VA).

Staining of the hyaloid vasculature

Following the removal of eyes, the sclera, choroids, and retina were dissected anteriorly from the optic nerve to limbus. The remaining whole mount specimen was stained with FITC-conjugated B4-lectin (1:100 dilution; Sigma, St. Louis, MO) to visualize the hyaloid vasculature. Whole mount specimens were viewed by fluorescence microscopy and images were captured in digital format using a Zeiss microscope (Carl Zeiss, Chester, VA). The dissection resulted, in most cases, in the loss of hyaloid artery and vasa hyaloidea propria vessels. However, the tunica vasculosa lentis vessels were clearly visible following lectin staining. These experiments were repeated at least three times with eyes from three different mice.

Western blot analysis

VEGF protein levels were determined by Western blotting of whole eye extracts prepared from P15 mice during OIR (5 days of hyperoxia and 3 days of normoxia) when maximum levels of VEGF are expressed (Wang et al., 2003). Mice were sacrificed by CO_2 inhalation, eyes were dissected, homogenized in RIPA buffer (10 mM HEPES pH 7.6, 142.5 mM KCl, 1% NP-40, and protease inhibitor cocktail; Roche Biochemicals), sonicated briefly, and incubated at 4°C for 20 min. Homogenates were centrifuged at 16,000 × *g* for 10 min at 4°C to remove insoluble material. Clear supernatants were transferred to a clean tube and protein concentrations were determined using DC protein assay (Bio-Rad). Approximately 20 μg of protein lysates was analyzed by SDS-PAGE (4–20% Tris-Glycin gel, Invitrogen, Carlsbad, CA) under reducing conditions and transferred to a Nitrocellulose membrane. Blot was incubated with a rabbit polyclonal anti-mouse VEGF antibody (1/2000; PeproTech, Rock hill, NJ), washed, and developed using a goat anti-rabbit HRP-conjugated secondary antibody (1:5000; Jackson Immunoresearch Laboratories, West Grove, PA) and ECL system (Amersham). The same blot was also probed with a monoclonal antibody to β-catenin (1:3000; BD transduction) to verify equal protein loading in all lanes.

Statistical analysis

Statistical differences between groups were evaluated with Student's unpaired *t* test (two-tailed). Mean ± standard deviation is shown.

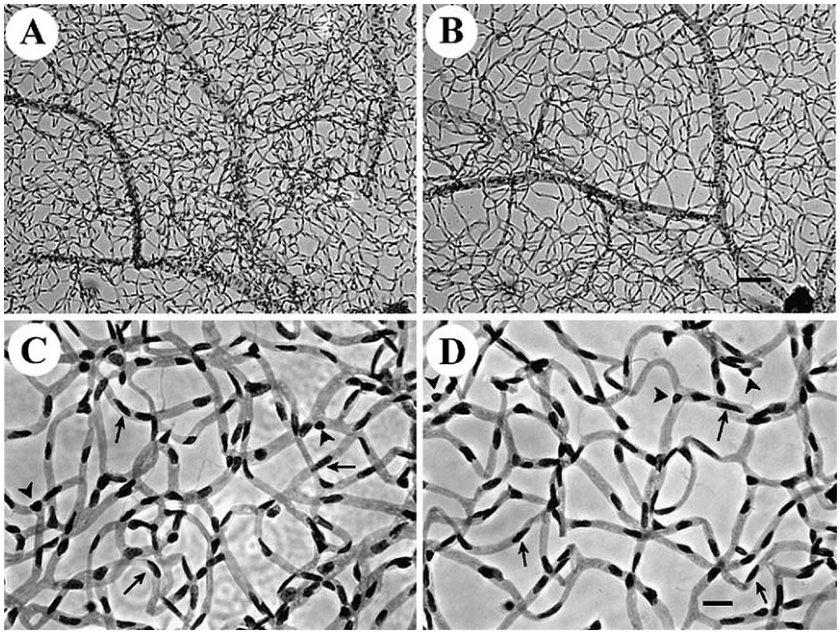

Fig. 1. Mouse retinal vasculature prepared by trypsin digestion technique. Retinas were obtained from P42 wild type (A and C) or bcl-2−/− mice (B and D). The arrows indicate endothelial cells while arrowheads show the pericytes lining the retinal capillaries. Please note the decreased number of capillary loops in the bcl-2−/− retina. Scale bar = 100 μm (A and B); 20 μm (C and D).

Results

bcl-2−/− mice exhibit decreased retinal vascular density

To compare retinal vascular densities in bcl-2+/+ and bcl-2−/− littermates, we prepared retinal trypsin digests and determined endothelial cells/pericyte (E/P) ratios as well as their densities. In whole mount retinal digests, the EC nuclei occur within the vessel wall, are large, oval, and weakly stained, and protrude luminally. Pericyte nuclei are darkly stained, small, round, and protrude laterally from the vessel wall. Fig. 1 shows retinal vessels prepared from postnatal day 42 (P42) wild type (A and C) and bcl-2−/− (B and D) mice. The retinal vasculature in bcl-2−/− mice exhibited less cellularity and fewer capillary loops, suggesting a decrease in retinal vascular density. This difference was also observed in retinal digests from P21 mice (Table 1). Table 1 shows the mean E/P ratios of retinal microvessels for wild type and bcl-2−/− mice. There was no significant difference in E/P ratios of wild type and bcl-2−/− mice at P21 and P42. Since the vascular density is lower in bcl-2−/− mice and the E/P ratio was similar to that of wild-type mice, we hypothesized that the number of both EC and pericytes in bcl-2−/− mice had decreased. We next determined the EC and pericyte densities. Tables 2 and 3 show the mean density of retinal EC and pericytes in wild type and bcl-2−/− mice, respectively. The mean densities of EC and pericytes were significantly lower in bcl-2−/− retinal microvessels at P21 and P42 when compared to wild-type mice. Therefore, the decreased retinal vascular density in bcl-2−/− mice is attributable to the reduction of the numbers of both EC and pericytes.

Development and remodeling of retinal vasculature was delayed in bcl-2−/− mice

The murine retinal vasculature develops postnatally. A superficial layer of vessels is formed during the first week of postnatal life (P7). These vessels sprout and penetrate the deep retina during the second and third week of postnatal life forming the deep retinal vascular plexuses by P21 (Dorrell et al., 2002). The course of retinal vessel sprouting and assembly can be readily visualized by PECAM-1 (a vascular endothelial cell marker) staining of whole mount retina preparations. The retinal vasculature continues undergoing remodeling and pruning up to 6 weeks after birth (Wang et al., 2003).

Table 1
E/P ratios in wild type and bcl-2−/− mice divided according to age (Mean ± SD)

Age, days	Wild type	Bcl-2-1−/−
21	1.97 ± 0.16(6)	2.20 ± 0.38(5)*
42	2.05 ± 0.31(8)	2.25 ± 0.51(6)*

The number of retinas (mice) counted is given in parentheses.
* No significant difference: $P > 0.05$.

Table 2
Number of endothelial cells per reticle square (100 μm^2) in wild type and bcl-2−/− mice divided according to age (density, Mean ± SD)

Age, days	Wild type	Bcl-2−/−
21	138.4 ± 10.0(6)	118.4 ± 13.3(5)*
42	114.0 ± 18.9(8)	93.6 ± 9.8(6)*

The number of retinas (mice) counted is given in parentheses.
* $P < 0.05$.

We compared retinal vascular development by PECAM-1 staining of whole mount retinas prepared from mice at different ages during postnatal vascular development. Figs. 2A and B show the developing retinal vessels in wild type and bcl-2−/− mice, respectively. As early as P7, there is a significant delay in development of retinal vasculature in bcl-2−/− mice. The formation of the superficial layer of vessels is normally complete, reaching the retinal periphery by P7. The development and maturation of vasculature is significantly delayed in the retinas of P7 bcl-2−/− mice (Figs. 2B and D) compared to wild-type littermates (Figs. 2A and C). We measured the distance that the retinal vessels had spread from the optic nerve head toward the retina periphery relative to the whole retina radius at P7. Fig. 2G shows there is a significant difference ($P < 0.01$) in the relative distance that the retinal vasculature spread from the optic nerve during the first week of life in bcl-2−/− mice compared to wild-type mice.

Previous studies have demonstrated a relationship between the developing retinal vasculature and retinal astrocytes. The astrocytes are a major component of the developing retinal vasculature providing the scaffolding for their organization, maturation, and remodeling. The roles served by astrocytes in inducing and controlling normal vessel development rely on their spreading across the retina ahead of the growing vessels (Fruttiger, 2002; Zhang and Stone, 1997). To determine whether this delay in the spreading of retinal vessels in bcl-2−/− mice was caused by the abnormal spreading of astrocytes, we examined the distribution of astrocytes by double staining of the whole mount retinas for GFAP and collagen IV. GFAP immuno-fluorescence labeling was used to identify astrocytes in developing retina vasculature. Figs. 2E and F show an area of the whole retina in P7 wild type and bcl-2−/− mice, respectively. The whole mount retina is viewed with the inner surface uppermost. Blood vessels and astrocytes spread from the optic disc toward the

Table 3
Number of pericytes per reticle square (100 μm^2) in wild type and bcl-2−/− mice divided according to age (density, Mean ± SD)

Age, days	Wild type	Bcl-2−/−
21	70.3 ± 3.3(6)	54.7 ± 8.1(5)*
42	56.0 ± 8.1(8)	43.0 ± 9.0(6)**

The number of retinas (mice) counted is given in parentheses.
* $P < 0.01$.
** $P < 0.05$.

peripheral margin of the retina. As demonstrated by GFAP staining at P7 in both wild type and bcl-2−/− mice, astrocytes have spread and reached the periphery of the retina. However, the spreading of the vessel was delayed in bcl-2−/− mice (Figs. 2A and B). Thus, the lag in development of retinal vessels in bcl-2−/− mice was not associated with impaired spreading of astrocytes in the vascular front.

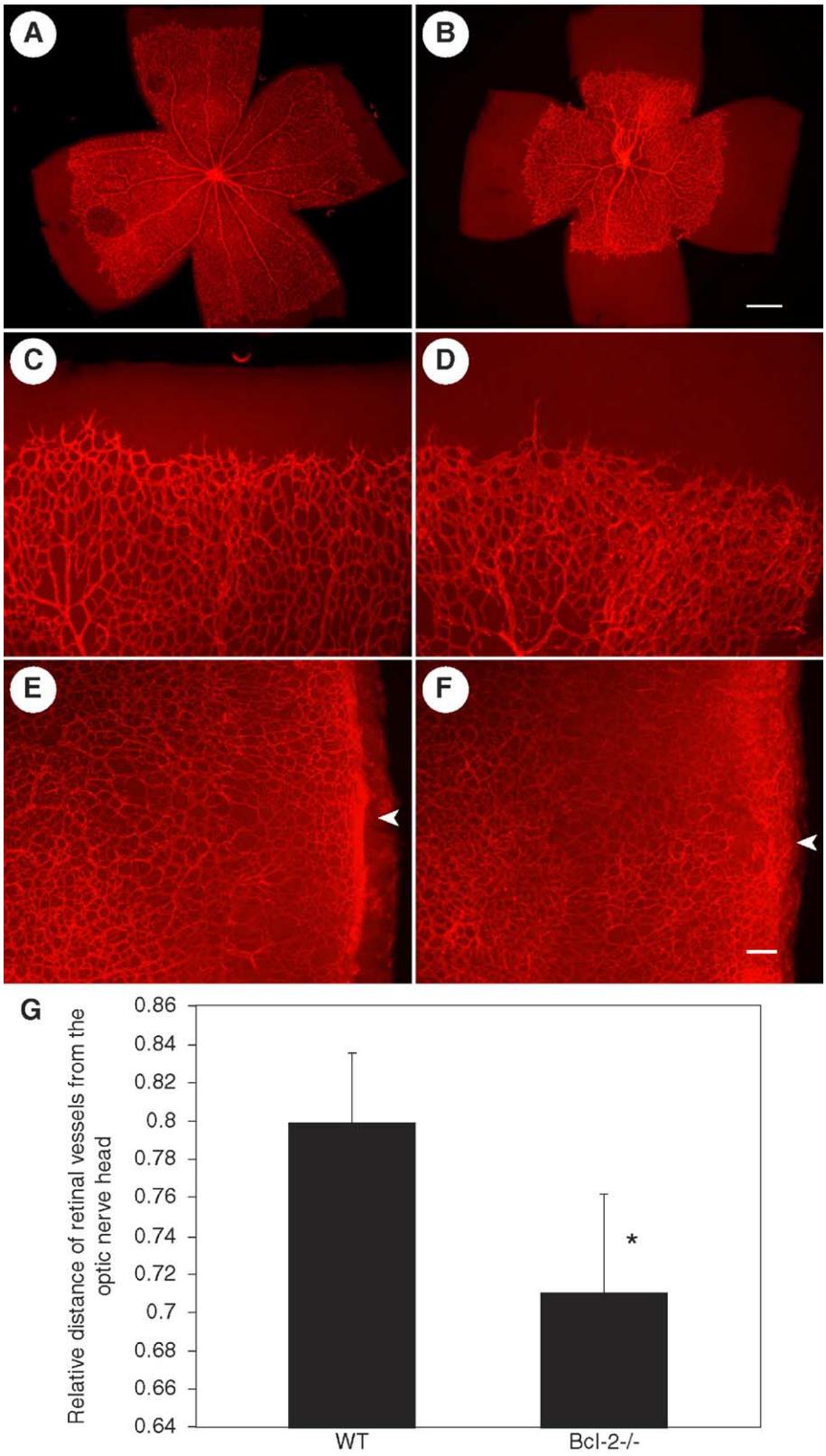

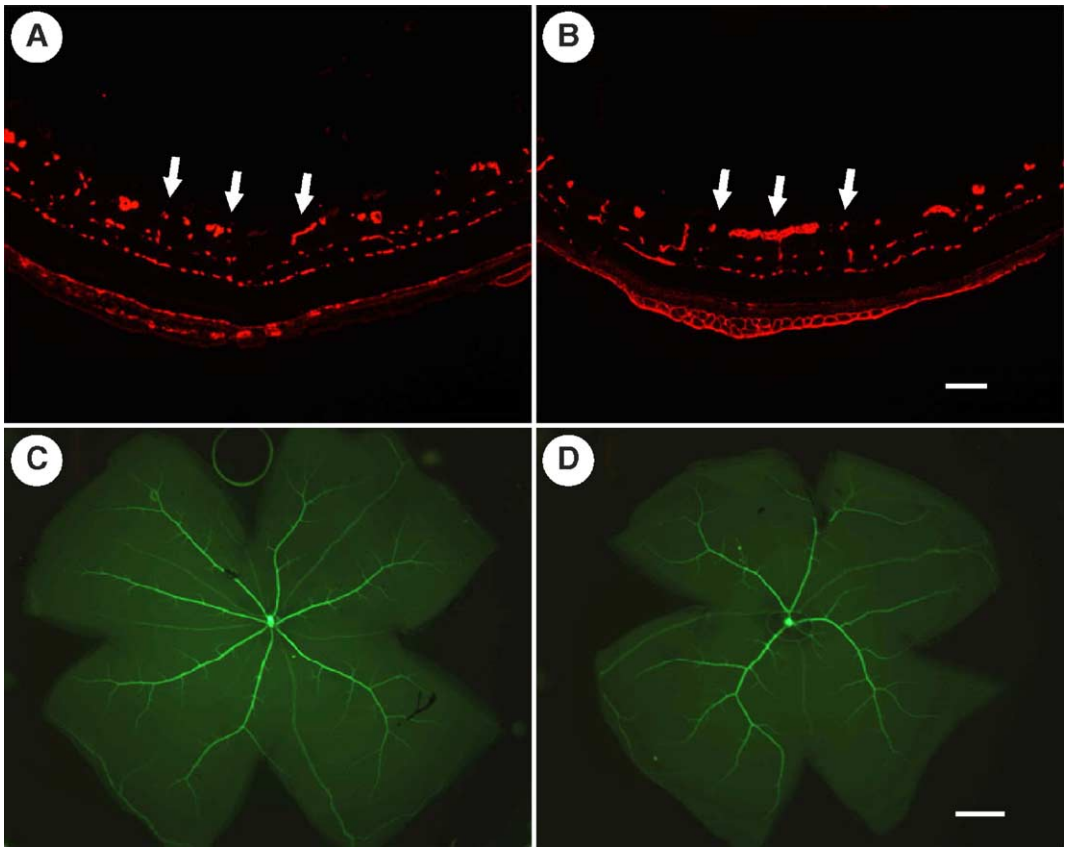

Fig. 3. Abnormal vascularization of the retina in the absence of bcl-2. Assessment of retinal vasculature was performed by collagen IV staining of frozen sections prepared from wild type (A) and bcl-2−/− (B) P42 mice. The arrows indicate the retinal vessels in the superficial layer. C and D show α-smooth muscle actin staining of retinal whole mounts from P21 wild type and bcl-2−/− mice, respectively. Please note the decreased number of vessels in the superficial and deep layers of bcl-2−/− retina (A and B) and the number of arteries branching from near the optic nerve, as well as abnormal secondary and tertiary branching (C and D). These experiments were repeated at least three times with eyes from three different mice. Scale bar = 100 μm (A and B); 500 μm (C and D).

To determine whether the formation of intermediate and deep layers of retinal vessels was affected, we examined frozen sections prepared from the eyes of P42 mice. Figs. 3A and B show type IV collagen staining of retinal vessels in cross-sections prepared from P42 wild type and bcl-2−/− mice, respectively. The bcl-2−/− retinas consistently exhibited a reduced number of vessels in all three layers of retinal vasculature (Fig. 3B) compared to wild-type mice (Fig. 3A). Previous studies demonstrated that the superficial layer of retinal vessels grows as a monolayer within the nerve fiber layer during the first 10 days after birth. During P7 to P9, the deep vascular plexus begins to form at the outer edge of the inner nuclear layer. This is followed by the formation of an intermediate vascular plexus between the primary and secondary vascular layer during the third postnatal week. Examination of the deep vascular plexuses on P14 and P21 showed a lower density of vessels in the deep layers of retinas from bcl-2−/− mice compared to wild-type mice (not shown). Therefore, the development of the retinal vascular plexuses was affected in its entirety in bcl-2−/− mice. This was further confirmed by α-smooth muscle actin staining of retina whole mounts. Figs. 3C and D show α-smooth muscle actin staining of whole mount retinas prepared from P21 wild type and bcl-2−/− mice, respectively. Anti-α-smooth muscle actin antibody mainly stains the major arteries covered by smooth muscle cells and not the capillaries (Fruttiger, 2002). We observed

Fig. 2. PECAM-1 and GFAP staining of the retinal whole mount prepared from wild type and bcl-2−/− mice. PECAM-1 (A–D) and GFAP (E and F) staining of the retinal whole mounts from wild type (A, C, E) and bcl-2−/− (B, D, F) P7 mice. The arrowheads (E and F) indicate the retinal periphery. Please note that the astrocytes have grown to the periphery of the retina in wild type and bcl-2−/− mice (E and F), but the blood vessels grow slower in bcl-2−/− mice compared to wild-type mice (C and D). The quantitative assessment of the distance retinal vessels spread relative to the radius of the retina at P7 is shown in G. Data in each bar are the mean distance blood vessels have spread from the optic nerve relative to the radius of each retina in five eyes of five mice in μm (error bars indicate standard deviation). Please note that the spreading of retinal vessels is significantly slower in bcl-2−/− mice compared to wild-type mice ($P < 0.01$). Scale bar = 500 μm (A and B); 100 μm (C–F).

a significant (~50%) decrease in the number of major arteries which branch off near the optic nerve. In addition, the degree and extent of secondary and tertiary branching are also compromised in bcl-2−/− retinal vasculature.

Increased apoptosis in the developing retinal vasculature of bcl-2−/− mice

The decrease in density of vascular cells observed in the bcl-2−/− mouse retinal vessels could be the result of increased apoptosis during retinal vascular development in the absence of bcl-2. Figs. 4A and B demonstrate TUNEL analysis of frozen sections prepared from P14 wild type and bcl-2−/− mice. We observed a significant increase in the number of apoptotic nuclei in the retinal vasculature of bcl-2−/− mice, mainly in the superficial layer at this stage. A similar result was observed upon staining of apoptotic vascular cells in whole mount retinas by an anti-active caspase-3 antibody (Figs. 4C and D). A quantitative assessment of these data is shown in Fig. 4E. During the counting of the caspase-positive cells, we took special care to only count cells that were directly associated with the

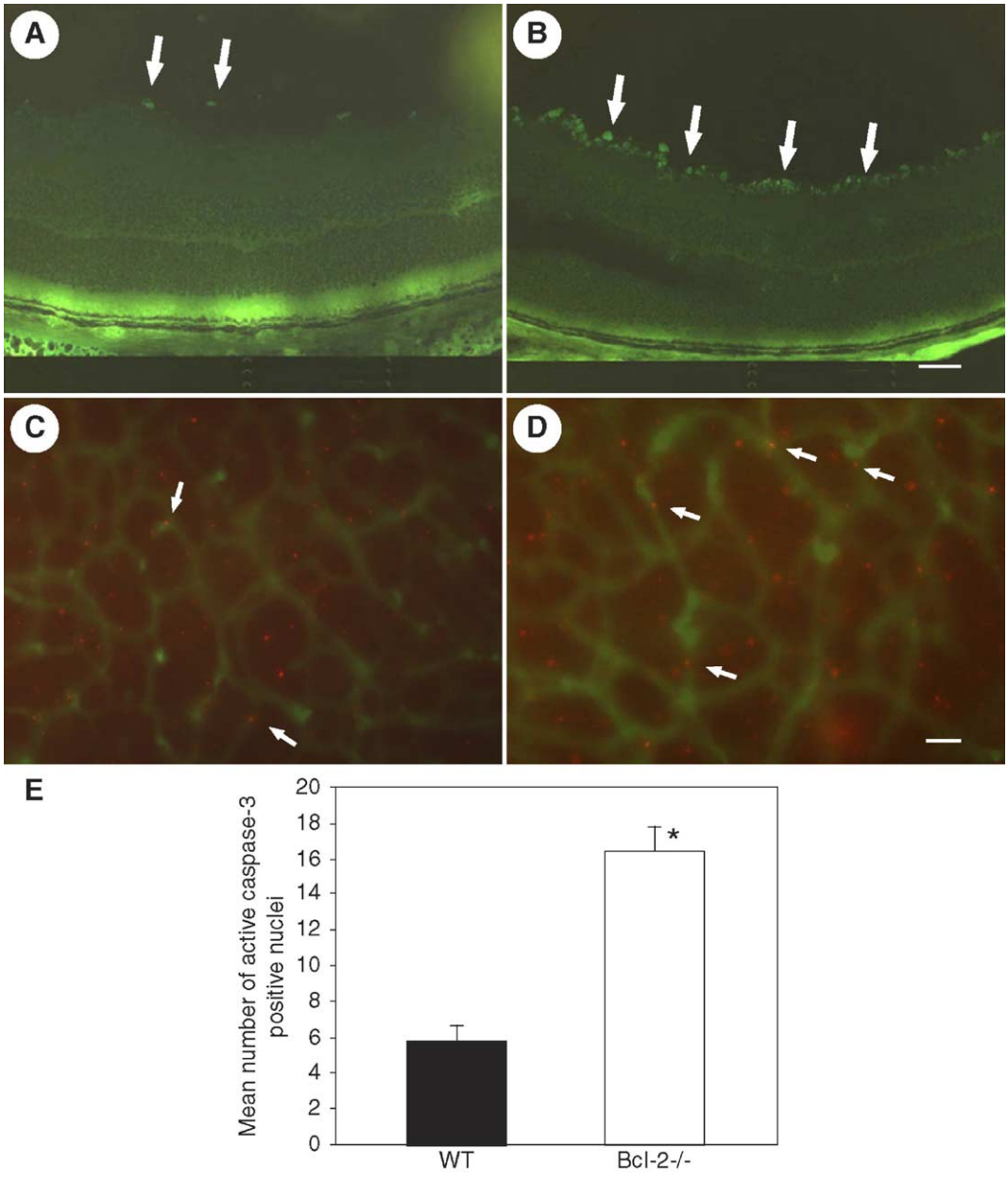

Fig. 4. Increased rates of apoptosis in retinal vasculature of bcl-2−/− mice. Frozen sections or whole mount retinas were subjected to apoptosis assays by TUNEL (A and B) or active caspase-3 staining (C and D). B4-lectin was used to visualize retinal vasculature in C and D. The quantitative assessments of apoptosis are shown in E. Data in each bar are the mean number of apoptotic nuclei counted in identical quadrants (100 μm^2) of each retina in five eyes of five mice (error bars indicate standard deviation). Please note a significant increase in the rate of apoptosis in bcl-2−/− retina compared to wild-type mice ($P < 0.01$). Scale bar = 50 μm (A and B); 20 μm (C and D). The arrows point to apoptotic cells.

vessels by examining different focal planes. However, we believe other cells which are positive but do not appear to be in direct contact with the vessels are apoptotic vascular cells that have not been phagocytized and cleared. It is unlikely that these cells are neuronal cells since the role of bcl-2 in the survival of neural retina is minimal (Cellerino et al., 1999; Dietz et al., 2001; Sharma, 2001). An approximately 3-fold increase in the number of apoptotic nuclei on the retinal vasculature of bcl-2−/− mice was observed compared to the wild-type mice. A significant difference in the number of apoptotic nuclei on the retinal vessel of bcl-2−/− mice compared to wild-type mice was also observed prior to 6 weeks of age (not shown). Thus, retinas from bcl-2−/− mice exhibit an increased vascular cell apoptosis compared to wild-type mice during retinal vascular development.

Increased proliferation in the developing retinal vasculature of bcl-2−/− mice

Previous studies in kidneys from bcl-2−/− mice demonstrated increased proliferation in conjunction with the increased amounts of apoptosis (Veis et al., 1993). To determine whether this was also the case in the retina, we examined cell proliferation in the retinal vasculature of wild type and bcl-2−/− mice. P14 wild type and bcl-2−/− mice were injected with BrdU, and labeled cells in retinal vascular whole mounts were detected by staining with anti-BrdU and collagen IV (stains blood vessels). P14 is a time point when the maximum amount of proliferation is observed in the wild-type mice (our unpublished data). Figs. 5A and B show retinal whole mounts from wild type and bcl-2−/− mice stained with anti-BrdU and collagen IV, respectively. We observed a significant increase in the number of BrdU-positive nuclei in the retinal vasculature of bcl-2−/− mice. Fig. 5C shows the quantitative assessment of these data. An approximately 2-fold increase in the number of BrdU-positive vascular cells was observed in the retinal vasculature of bcl-2−/− mice compared to the wild-type mice. Retinal vascular proliferation diminishes significantly with time. We consistently see very little, if any, proliferation in retinal vasculature of P21 wild-type mice (our unpublished data). However, there is a significant amount of proliferation in retinal vasculature from P21 bcl-2−/− mice compared to wild-type mice (not shown).

Regression of hyaloid vessels was not affected in the bcl-2−/− mice

The pupillary membrane and hyaloid vessels, hyaloid arteries, tunica vasculosa lentis, and vasa hyaloidea propria,

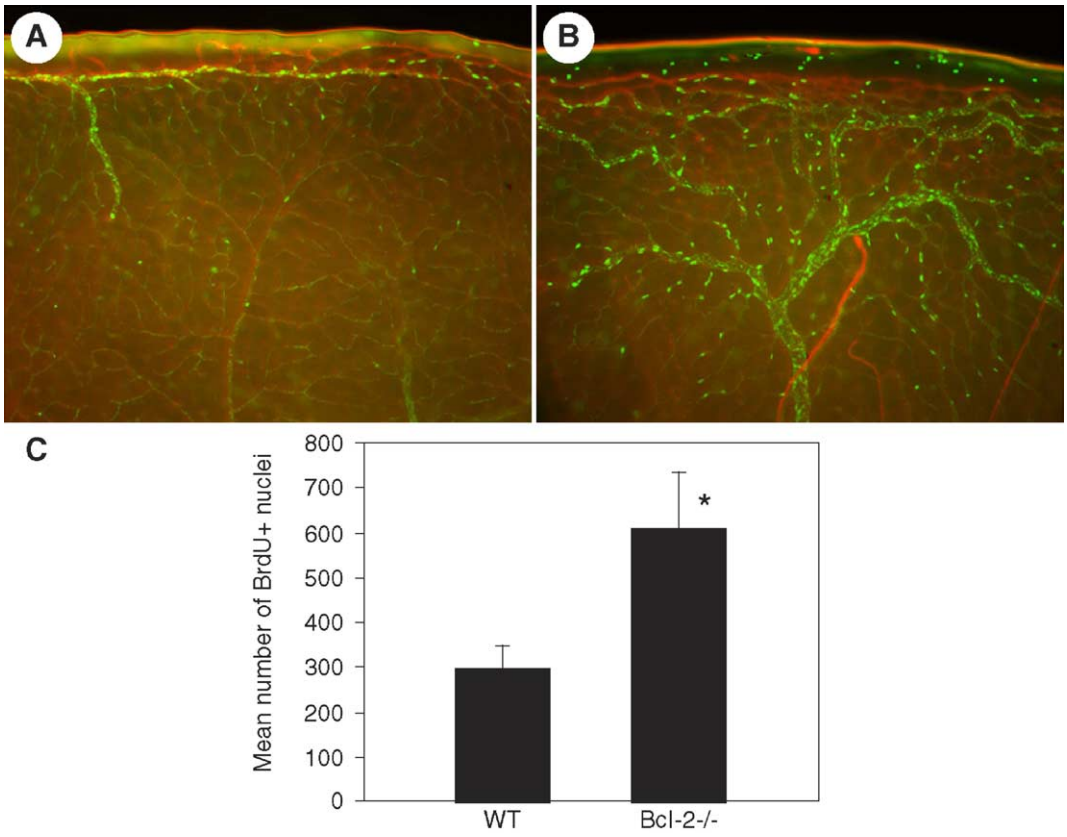

Fig. 5. Enhanced cell proliferation in retinal vasculature of bcl-2−/− mice. Proliferating cells were labeled by BrdU and detected using an antibody to BrdU as described in Materials and methods. Collagen IV staining was used to visualize the vasculature. Quantitative assessment of cell proliferation on the retinal vessels at P14 is shown in C. Data in each bar are the mean number of BrdU+ cells counted in each retina in five eyes of five mice (error bars indicate standard deviation). Please note that the number of proliferating cells is significantly higher in bcl-2−/− retinas compared to wild type ($P < 0.01$). Scale bar = 100 μm.

provide nourishment to the immature lens, retina, and vitreous (Ito and Yoshioka, 1999). However, they regress during the later stages of ocular development. Fig. 6 shows the staining of the vasculature in whole mount ocular specimens prepared from wild type and bcl-2−/− mice at 1, 2, and 4 weeks of age. We observed a significant amount of hyaloid vessels (mainly tunica vasculosa lentis) in wild type and bcl-2−/− mice by 1 week of age (Figs. 6A and B). However, these vessels regressed similarly in the wild type and bcl-2−/− mice by 2 and 4 weeks of age (Figs. 6C–F), and by 6 weeks of age complete regression of the hyaloid vessels was noted (not shown). Therefore, absence of bcl-2 does not appear to impact the regression of hyaloid vessels. However, our results do not exclude possible structural and functional differences in the development of hyaloid vessels in bcl-2−/− mice.

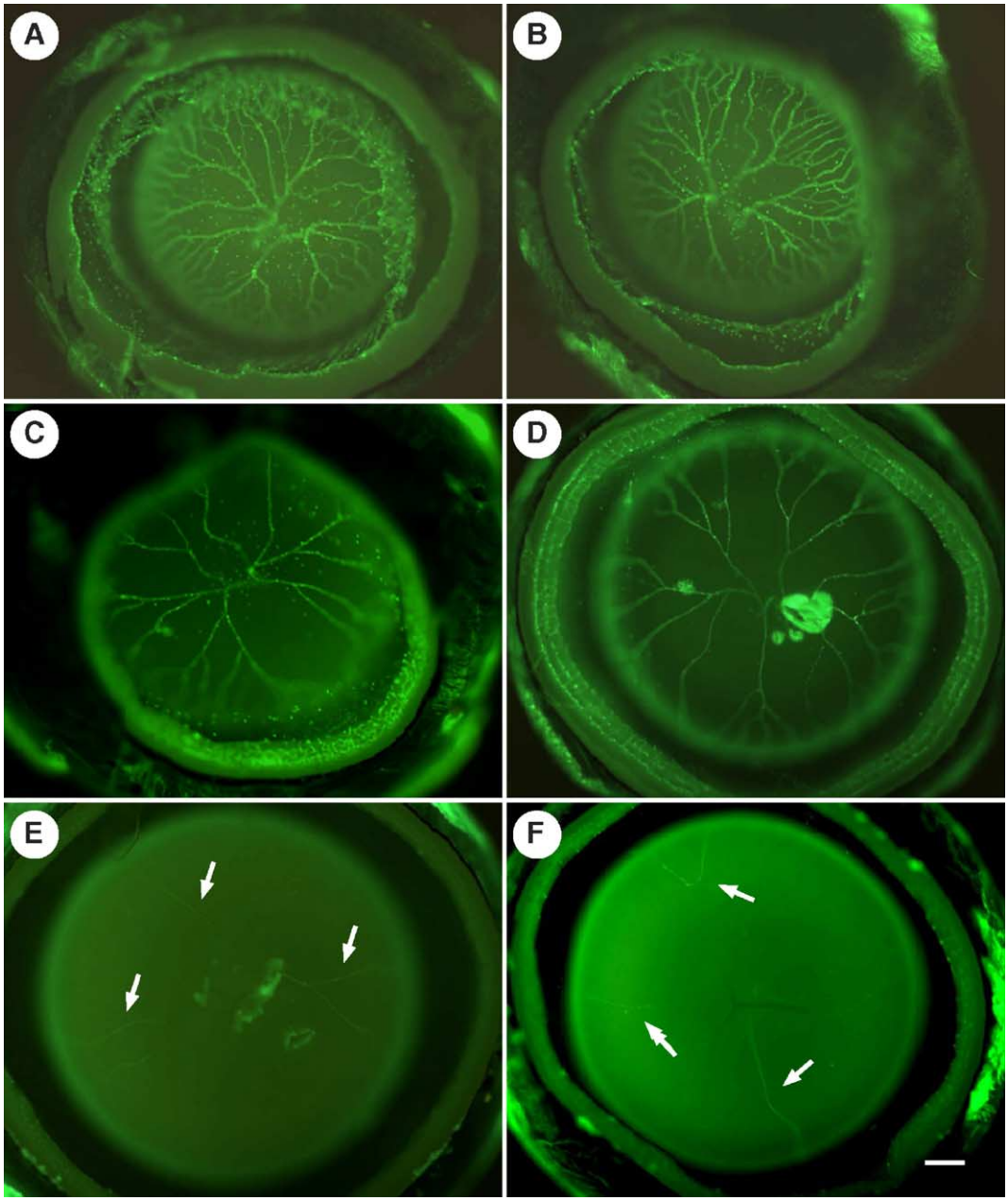

Fig. 6. Assessment of hyaloid vasculature in wild type and bcl-2−/− mice. The whole mount staining of hyaloid vasculature from wild type (A, C, and E) and bcl-2−/− (B, D, and F) mice at 1 week (A and B), 2 weeks (C and D), and 4 weeks (E and F) was prepared as described in Materials and methods. Please note similar degrees of vascularization in wild type and bcl-2−/− mice at all time points. Scale bar = 200 μm. Arrows point to vessels which have not regressed at 4 weeks. These experiments were repeated at least three times with eyes from three different mice. The areas of B4-lectin over-staining in D and E are non-specific staining due to mechanical manipulation of tissue during preparation of specimens.

The developing retinal vasculature of bcl-2−/− mice is similarly sensitive to hyperoxia-mediated vessel obliteration compared to wild-type mice during oxygen-induced ischemic retinopathy

Retinal vascularization is tightly coupled with its oxygen needs and exhibits an inherent sensitivity to fluctuations in oxygen levels during the early stages of retinal vascularization. This predisposes the developing retina to retinopathy of prematurity, which results in ischemia-driven neovascularization of the retina and loss of vision upon exposure to hyperoxia. The mouse model of oxygen-induced ischemic retinopathy (OIR) is a highly reproducible model for studying all aspects of angiogenesis. In this model, P7 mice are exposed to 75% oxygen for 5 days, and then returned to room air for 5 days. The exposure of developing retina vasculature to high oxygen prevents growth of additional vessels and promotes loss of existing vessels due to diminished expression of VEGF, and perhaps bcl-2 (Wang et al., 2003). Therefore, when animals are returned to room air, the retina becomes ischemic and promotes growth of new vessels, which grow into the vitreous.

We next compared the response of bcl-2−/− and wild-type mice to oxygen-induced ischemic retinopathy. Figs. 7A and B show whole mount PECAM-1 staining of the retinal vasculature in P17 mice subjected to OIR. In wild-type mice, the retinal non-perfused areas were reduced, and by P17, these retinas formed an increasing number of new vessels. In contrast, in retinas from P17 bcl-2−/− mice, significant vascularization of the non-perfused area and growth of new vessels were not observed. To determine whether the sensitivity of retinal vascular to hyperoxia is affected in the absence of bcl-2, we examined retinal non-perfused areas in P12 retinas, when maximum vessel obliteration is observed (5 days of hyperoxia). Fig. 7C shows the quantitative measurements of non-perfused area relative to the whole retina area in wild type and bcl-2−/− mice. These mice showed a similar degree of sensitivity to hyperoxia-mediated vessel obliteration at P12. Upon expo-

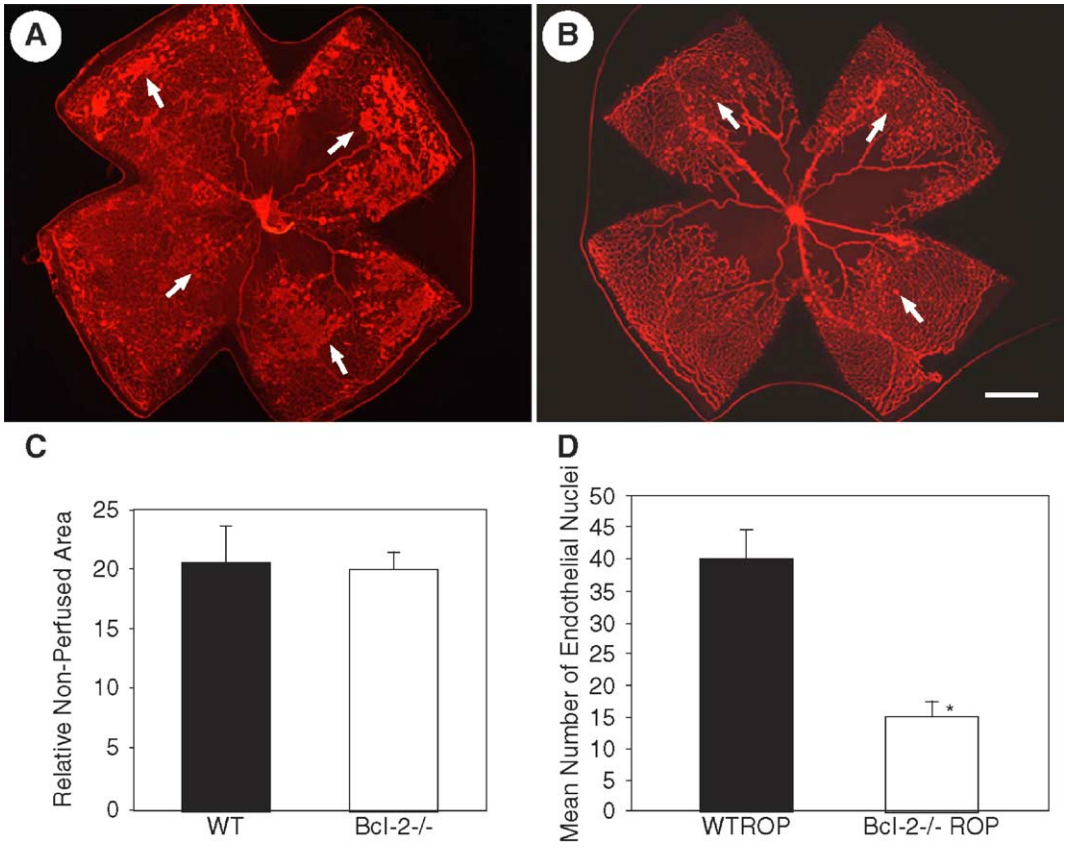

Fig. 7. Quantitative assessment of neovascularization in P 17 mice exposed to a cycle of hyperoxia and room air (OIR). A and B are PECAM-1-stained whole mount retinas prepared from wild type and bcl-2−/− P17 mice, respectively. The arrows indicate growth of new vascular tufts which are significantly diminished in bcl-2−/− mice. The quantitative assessment of non-perfused area at P12 (5 days of hyperoxia) is shown in C. Data in each bar are the mean non-perfused area relative to the whole area of each retina in five eyes of five mice (error bars indicate standard deviation). Please note that there is no significant difference in the degree of vessel obliteration in response to hyperoxia in wild type and bcl-2−/− mice ($P = 0.73$). The number of vascular cell nuclei present on the vitreous side of the retina penetrating the inner limiting membrane was determined as described in Materials and methods at P17 and presented in D. Data in each bar are the mean number of vascular cell nuclei in five eyes of five mice (error bars indicate standard deviation). Please note that there is a significant decrease in the degree of retinal neovascularization in bcl-2−/− mice compared to wild-type mice ($P < 0.01$). Scale bar = 500 μm.

sure to room air (5 days), ischemia drives the growth of new vessels, which vascularize the non-perfused areas and grow new vessels into the vitreous. During exposure to normoxia, neovascularization occurs in the retinal periphery and sprouting of new vessels from the existing larger vessels in the non-perfused area is observed which is dependent on the expression of VEGF and bcl-2 (Wang et al., 2003; and Figs. 7A and B). This results in re-establishment of vasculature in the non-perfused area and growth of new vessels into the vitreous (preretinal vessels) by P17.

Quantification of pre-retinal neovascularization

Quantification of pre-retinal neovascularization on P17 mice (when maximum pre-retinal neovascularization occurs) was performed as described previously (Wang et al., 2003). Briefly, 6-μm-thick serial sections, each separated by at least 40 μm, were obtained from the region around the optic nerve. The sections were stained with hematoxylin and PAS and examined in masked fashion for the presence of neovascular cell nuclei projecting into the vitreous from the retina. The neovascular cell nuclei score was defined as the mean number of neovascular nuclei per section found in eight sections (four on each side of the optic nerve) per eye. Fig. 7D shows the mean number of vascular cell nuclei projecting into the vitreous of eyes from wild type and bcl-2−/− mice. There were significantly fewer vascular cell nuclei detected in the P17 bcl-2−/− mice compared to the wild-type mice. This is mainly attributed to the lack of bcl-2, which is required for survival of vascular cells during angiogenesis. Therefore, expression of bcl-2 contributes to neovascularization of retinas in response to ischemia.

VEGF expression is not affected following OIR in the absence of bcl-2

To determine whether the inability of retinas from bcl-2−/− mice to undergo neovascularization in response to ischemia was due to lack of VEGF expression, we examined VEGF levels in retinas from P15 wild type and bcl-2−/− mice (5 days of hyperoxia and 3 days of normoxia). VEGF expression is maximally induced during OIR at P15 (Wang et al., 2003). Fig. 8 shows a Western blot of protein prepared from whole eye extracts of P15 wild type and bcl-2−/− mice during OIR. We observed similar levels of VEGF expression in eyes from P15 wild type and bcl-2−/− mice during OIR. Therefore, the inability of retinal neovascularization in the absence of bcl-2 was not due to lack of VEGF expression.

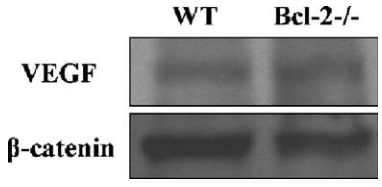

Fig. 8. Assessment of VEGF levels in eyes from wild type and bcl-2−/− mice. Eye extracts prepared from wild type and bcl-2−/− P15 mice (5 days of hyperoxia and 3 days of normoxia) were analyzed by SDS-PAGE and Western blotting as described in Materials and methods. Please note expression of similar levels of VEGF in wild type and bcl-2−/− mice. β-catenin was used for loading control. These experiments were repeated at least three times with eyes from three different mice.

Lack of bcl-2 does not affect the development of neural retina

The potential contribution of bcl-2 to the development of the neural retina has been previously studied. Previous studies indicated that the survival of retinal ganglion cells is not compromised, both during early development and axotomy-induced apoptosis in adult mice, by the absence of bcl-2 (Cellerino et al., 1999; Dietz et al., 2001). Furthermore, bcl-2 expression is not altered during retinal degeneration (Sharma, 2001). We next examined retinal sections prepared from wild type and bcl-2−/− mice at 3 weeks and 6 weeks of age (Fig. 9). The thickness, the cellularity, and the organization of retinal layers were minimally affected in bcl-2−/− mice compared to wild-type mice. Therefore, our data further confirm previous studies indicating that the development of the neural retina is not compromised in the absence of bcl-2.

Discussion

Programmed cell death (apoptosis) of vascular cells plays an important role in controlling the morphology and cellular components of the blood vessels (Pollman et al., 1999; Segura et al., 2002; Walsh et al., 2000; Wang et al., 2003). Bcl-2 regulates apoptosis and is essential for viability of vascular cells in vitro and in vivo (Biroccio et al., 2000; Matsushita et al., 2000; Nor et al., 2001; Segura et al., 2002). However, the physiological role bcl-2 plays during vascular development and remodeling requires further delineation. Here we demonstrate that bcl-2−/− mice exhibit a decreased retinal vascular density, which starts at the early stages of the developing retinal vasculature resulting in a compromised vasculature in adult mice independent of the developing neural retina. The retinal vasculature of bcl-2−/− mice exhibited a similar susceptibility to hyperoxia-induced vessel obliteration compared to wild-type mice. However, the retinal vasculature of bcl-2−/− mice was protected from hypoxia-induced retinal neovascularization. Thus, even though VEGF is expressed in these mice following OIR, hypoxia-induced neovascularization does not occur in the absence of bcl-2 expression. Our results indicate that bcl-2 is required for appropriate development of retinal vasculature and ischemia-driven neovascularization.

Although the expression and role of bcl-2 were examined in the developing retina, the main interest was in bcl-2's role in the survival of neuronal cells (Cellerino et al., 1999; Dietz

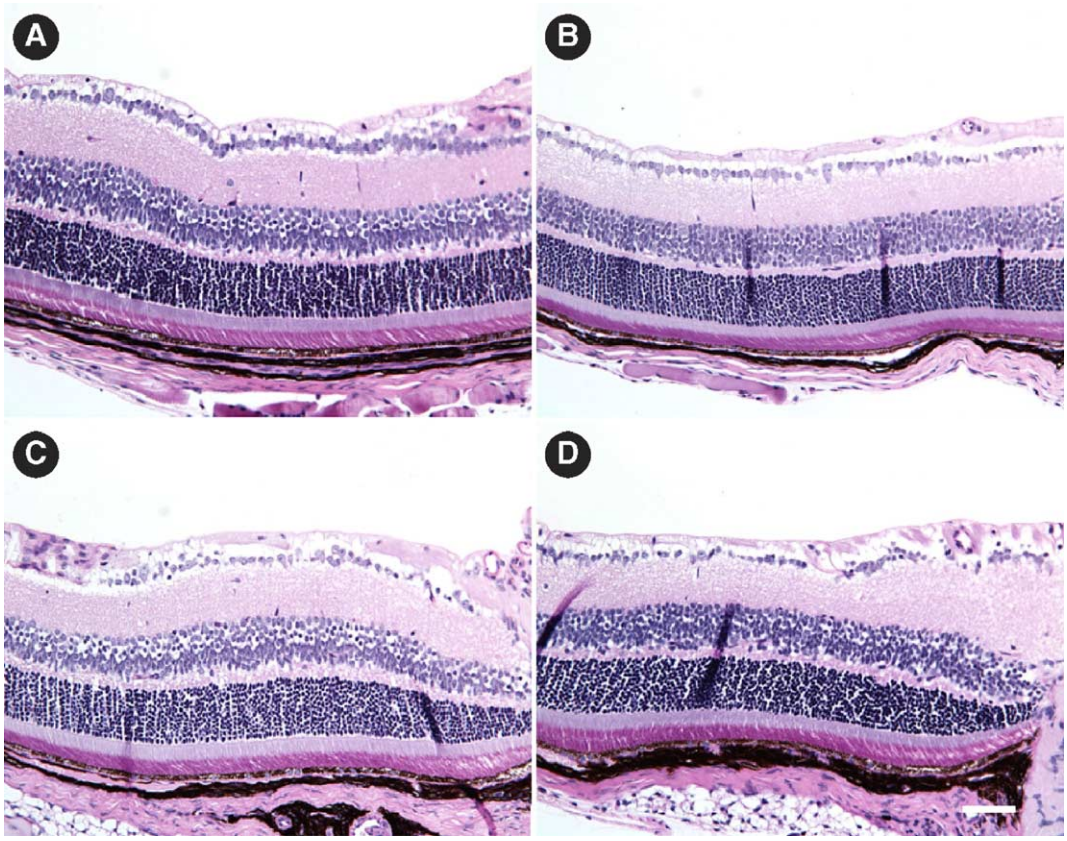

Fig. 9. Comparison of retinal sections prepared from wild type and bcl-2−/− mice. Eyes were enucleated, fixed, and paraffin embedded as described in Materials and methods for quantitative assessment of retinal neovascularization. Sections (6 μm) prepared from the same areas were hematoxylin- and PAS-stained, and photographed in digital format (A and C; wild type) (B and D; bcl-2−/−). These experiments were repeated at least three times with eyes from three different mice at 3 weeks (A and B) or 6 weeks (C and D) of age. Please note that the thickness, the cellularity, and the organization of the retina layers are not compromised in the absence of bcl-2.

et al., 2001; Martinou et al., 1994; Middleton et al., 1998; Sharma, 2001; Strettoi and Volpini, 2002). Bcl-2 expression is required for survival of primary motoneurons and peripheral neurons soon after the period of naturally occurring cell death (Cellerino et al., 1999). The physiological expression of bcl-2 is not affected during retinal degeneration. However, ectopic expression of bcl-2 in photoreceptor cells results in their preservation (Nir et al., 2000; Sharma, 2001). Therefore, the role of bcl-2 in the survival and development of neuronal components of the retina, in contrast to the developing retinal vasculature, appears to be minimal.

Apoptosis plays an important role during lumen formation, remodeling, and regression of vasculature during development (Peters et al., 2002; Pollman et al., 1999; Schechner et al., 2000; Segura et al., 2002; Walsh et al., 2000). The important role of bcl-2 in angiogenesis has been demonstrated by its enhanced production by angiogenic factors, while factors that inhibit angiogenesis generally down-regulate bcl-2 expression. Therefore, appropriate expression of bcl-2 may play a central role during vascular development and angiogenesis. Bcl-2−/− mice retina exhibited a reduced vascular density mainly due to excessive loss of vascular cells, including EC and smooth muscle cells/pericytes. This was apparent at very early stages of retinal vascularization where a significant delay in progression and remodeling of the developing vasculature was observed (Fig. 2). In addition, a significant increase in the rates of cell proliferation and apoptosis was observed in the developing vasculature of the bcl-2−/− retinas (Figs. 4 and 5). This is consistent with our previous observations in the developing kidney where excessive apoptosis was accompanied by increased compensatory proliferation (Veis et al., 1993). Thus, expression of bcl-2 by vascular cells is essential for their integrity and their ability to form blood vessels.

Bcl-2 is an important modulator of EC survival, and its expression in these cells enhances their ability to not only form more stable vessels, but also promote recruitment of vascular supporting cells in vivo (Schechner et al., 2000, 2003). In addition, appropriate apoptosis is essential for the ability of EC to branch and form lumen in vitro (Pollman et al., 1999; Segura et al., 2002; Walsh et al., 2000). Bcl-2 expression in smooth muscle cells is also essential for their survival and proliferative activity (Hata et al., 2001; Li et al., 1998). These observations are consistent with our data in the retinal vasculature from bcl-2−/− mice. Here we detect a reduced number of EC and pericytes, as well as a significant

decrease in the number of major arteries branching off from the area near the optic nerve. In addition, vascular smooth muscle cells release several factors, including VEGF, in order to maintain bcl-2 levels in EC promoting their survival in the vasculature (Hata et al., 2001). Therefore, expression of bcl-2 in EC and pericytes is essential for the development and functioning of the retinal vasculature.

To determine the potential role of bcl-2 in the regression of hyaloid vessels, an apoptosis-dependent process, we examined the hyaloid vasculature at different postnatal days (Fig. 6). The pupillary membrane and hyaloid vessels (hyaloid arteries, tunica vasculosa lentis, and vasa hyaloidea propria) provide nourishment to the immature lens, retina, and vitreous (Ito and Yoshioka, 1999). However, they are known to regress during the later stages of ocular development by apoptosis. The contribution of bcl-2 to these processes has not been previously addressed. Our results show that the regression of hyaloid vessels, mainly the tunica vasculosa lentis, was not significantly affected in bcl-2−/− mice compared to wild-type mice (Fig. 6). Therefore, the regression of ocular embryonic vessels is not compromised in the absence of bcl-2.

The mouse oxygen-induced ischemic retinopathy is a highly reproducible model of neovascularization and is extensively utilized for testing antiangiogenic activity of many compounds. In this model, the P7 mice and their mother are exposed to 75% oxygen for 5 days. The high level of oxygen inhibits VEGF expression, a factor that promotes survival and proliferation of EC, as well as astrocytes, during vascularization of the retina. This results in obliteration of the recently formed vessels by apoptosis and prevention of new vessel growth. Our results showed similar levels of vessel obliteration in bcl-2−/− and wild type retinal vasculature. Thus, the lack of bcl-2 does not affect retinal vasculature sensitivity to high oxygen. This is consistent with a role demonstrated for other bcl-2 family members with pro-apoptotic activity in hyperoxia-induced cell death (Budinger et al., 2002).

When animals are returned to room air, the retina becomes ischemic because of excessive loss of retinal vessels during hyperoxia. This signals production of VEGF, which promotes proliferation and survival of endothelial cells, perhaps by up-regulation of bcl-2, resulting in formation of new vessels (Wang et al., 2003). However, the extreme sensitivity of astrocytes to normoxia, following exposure to hyperoxia, results in loss of astrocytes, which are important not only in the formation of retinal vessels but also for their function (Stone et al., 1996). Therefore, the newly formed vessels, which are functionally abnormal, invade the vitreous and leak resulting in loss of vision. Our data demonstrate that the bcl-2−/− retinal vasculature is significantly protected from ischemia-driven neovascularization during OIR. The ability of VEGF to promote formation of new vessels is mediated through up-regulation of bcl-2 expression (Gerber et al., 1998; Nor et al., 1999). Our results demonstrate that the lack of bcl-2 does not affect expression of VEGF in response to normoxia. Therefore, bcl-2 expression is an essential component of the newly forming vessels during oxygen-induced ischemic retinopathy.

In summary, bcl-2 expression is essential during vascular development and angiogenesis. In its absence, the development of retinal vasculature is compromised and fails to elicit a neovascular response during OIR. The essential role of bcl-2 in ischemia-driven angiogenesis makes it a suitable target for inhibition and/or promotion of angiogenesis under such conditions. Therefore, inhibition of bcl-2 expression and/or survival activity may provide an effective target for treatment of retinopathy of prematurity as well as other diseases whose pathological manifestation is dependent on ischemia-driven neovascularization.

Acknowledgments

This research was supported in part by National Institutes of Health grants AR45599 and EY13700. NS is a recipient of a Career Development Award from the Research to Prevent Blindness Foundation. CMS is supported by the Solomon Papper MD Young Investigator Grant of the National Kidney Foundation and the PKD Foundation.

References

Biroccio, A., Candiloro, A., Mottolese, M., Sapora, O., Albini, A., Zupi, G., Del Bufalo, D., 2000. Bcl-2 overexpression and hypoxia synergistically act to modulate vascular endothelial growth factor expression and in vivo angiogenesis in a breast carcinoma line. FASEB J. 14, 652–660.

Budinger, G.R.S., Tso, M., McClintock, D.S., Dean, D.A., Sznajder, J.I., Chandel, N.S., 2002. Hyperoxia-induced apoptosis does not require mitochondrial reactive oxygen species and is regulated by Bcl-2 proteins. J. Biol. Chem. 277, 15654–15660.

Cellerino, A., Michaelidis, T., Barski, J.J., Bahr, M., Thoenen, H., Meyer, M., 1999. Retinal ganglion cell loss after the period of naturally occurring cell death in Bcl-2−/− mice. NeuroReport 10, 1091–1095.

Dhanabal, M., Ramchandran, R., Waterman, M.J.F., Lu, H., Knebelmann, B., Segal, M., Sukhatme, V.P., 1999. Endostatin induces endothelial cell apoptosis. J. Biol. Chem. 274, 11721–11726.

Dietz, G.P., Kilic, E., Bahr, M., Isenmann, S., 2001. Bcl-2 is not required in retinal ganglion cells surviving optic nerve axotomy. NeuroReport 12, 3353–3356.

Dorrell, M.I., Aguilar, E., Friedlander, M., 2002. Retinal vascular development is mediated by endothelial filopodia, a pre-existing astrocytic template and specific R-cadherin adhesion. Invest. Ophthalmol. Visual Sci. 43, 3500–3510.

Fruttiger, M., 2002. Development of the mouse retinal vasculature: angiogenesis versus vasculogenesis. Invest. Ophthalmol. Visual Sci. 43, 522–527.

Gerber, H.P., Dixit, V., Ferrara, N., 1998. Vascular endothelial growth factor induces expression of the antiapoptotic proteins Bcl-2 and A1 in vascular endothelial cells. J. Biol. Chem. 273, 13313–13316.

Hata, S., Fukuo, K., Morimoto, S., Eguchi, Y., Tsujimoto, Y., Ogihara, T., 2001. Vascular smooth muscle maintains the levels of Bcl-2 in endothelial cells. Atherosclerosis 154, 309–316.

Ito, M., Yoshioka, M., 1999. Regression of the hyaloid vessels and papillary membrane of the mouse. Anat. Embryol. 200, 403–411.

Jimenez, B., Volpert, O.V., Crawford, S.E., Febbraio, M., Silverstein, R.L., Bouck, N., 2000. Signals leading to apoptosis-dependent inhibition of neovascularization by thrombospondin-1. Nat. Med. 6, 41–48.

Karsan, A., Yee, E., Poirier, G.G., Zhou, P., Craig, R., Harlan, J.M., 1997. Fibroblast growth factor-2 inhibits endothelial cell apoptosis by Bcl-2-dependent and independent mechanisms. Am. J. Pathol. 151, 1775–1784.

Li, W., Liu, X., He, Z., Yanoff, M., Jian, B., Ye, X., 1998. Expression of apoptosis regulatory genes by retinal pericytes after rapid glucose reduction. Invest. Ophthalmol. Visual Sci. 39, 1535–1543.

Longoni, B., Boschi, E., Demontis, G.C., Ratto, G.M., Mosca, F., 2001. Apoptosis and adaptive responses to oxidative stress in human endothelial cells exposed to cyclosporine A correlate with Bcl-2 expression levels. FASEB J. 15, 731–740.

Martinou, J.C., Dubois-Dauphin, M., Staple, J.K., Rodriguez, I., Frankowski, H., et al., 1994. Overexpression of Bcl-2 in transgenic mice protects neurons from naturally occurring cell death and experimental ischemia. Neuron 13, 1017–1030.

Matsushita, H., Morishita, R., Nata, T., Aoki, M., Nakagami, H., Taniyama, Y., Yamamoto, K., Higaki, J., Yasufumi, K., Ogihara, T., 2000. Hypoxia-induced endothelial apoptosis through nuclear factor-(B (NF-κB)-mediated Bcl-2 suppression in vivo evidence of NF-κB in endothelial cell regulation. Circ. Res. 86, 974–981.

Middleton, G., Pinon, L.G.P., Wyatt, S., Davies, A.M., 1998. Bcl-2 accelerates the maturation of early sensory neurons. J. Neurosci. 18, 3344–3350.

Nir, I., Kedzierski, W., Chen, J., Travis, G.H., 2000. Expression of Bcl-2 protects against photoreceptor degeneration in *retinal degeneration slow (rds)* mice. J. Neurosci. 20, 2150–2154.

Nor, J.E., Christensen, J., Mooney, D.J., Polverini, P.J., 1999. Vascular endothelial growth factor (VEGF)-mediated angiogenesis is associated with enhanced endothelial cell survival and induction of Bcl-2 expression. Am. J. Pathol. 154, 375–384.

Nor, J.E., Christensen, J., Liu, J., Peters, M., Mooney, D.J., Strieter, R.M., Polverini, P.J., 2001. Up-regulation of Bcl-2 in microvascular endothelial cells enhances intratumoral angiogenesis and accelerates tumor growth. Cancer Res. 61, 2183–2188.

Peters, K., Troyer, D., Kummer, S., Kirkpatrick, C., Rauterberg, J., 2002. Apoptosis causes lumen formation during angiogenesis in vitro. Microvasc. Res. 64, 334–338.

Pollman, M.J., Naumovski, L., Gibbons, G.H., 1999. Endothelial cell apoptosis in capillary network remodeling. J. Cell. Physiol. 178, 359–370.

Schechner, J.S., Nath, A.K., Zheng, L., Kluger, M.S., Hughes, C.C.W., Sierra-Honigmann, M.R., Lorber, M.I., Tellides, G., Kashgarian, M., Bothwell, A.L.M., Pober, J.S., 2000. In vivo formation of complex microvessels lined by human endothelial cells in an immunodeficient mouse. Proc. Natl. Aca. Sci. U. S. A. 97, 9191–9196.

Schechner, J.S., Crane, S.K., Wang, F., Szeglin, A.M., Tellides, G., Lorber, M.I., Bothwell, A.L.M., Pober, J.S., 2003. Engraftment of a vascularized human skin equivalent. FASEB J. 17, 2250–2256.

Segura, I., Serrano, A., De Buitrago, G.G., Gonzalez, M.A., Abad, J.L., Claveria, C., Gomez, L., Bernad, A., Martinez-a, C., Riese, H.H., 2002. Inhibition of programmed cell death impairs in vitro vascular-like structure formation and reduces in vivo angiogenesis. FASEB J. 16, 833–841.

Sharma, R.K., 2001. Bcl-2 expression during the development and degeneration of RCS rat retinae. Dev. Brain Res. 132, 81–86.

Sorenson, C.M., 2004. Bcl-2 family members and disease. Biochim. Biophys. Acta 1644, 169–177.

Stone, J., Chan-Ling, T., Pe'er, J., Itin, A., Gnessin, H., Keshet, E., 1996. Roles of vascular endothelial growth factor and astrocyte degeneration in the genesis of retinopathy of prematurity. Invest. Ophthalmol. Visual Sci. 37, 290–299.

Strettoi, E., Volpini, M., 2002. Retinal organization in the Bcl-2-overexpressing transgenic mouse. J. Comp. Neurol. 446, 1–10.

Veis, D.J., Sorenson, C.M., Shutter, J.R., Korsmeyer, S.J., 1993. Bcl-2-deficient mice demonstrate fulminant lymphoid apoptosis, polycystic kidneys, and hypopigmented hair. Cell 75, 229–240.

Walsh, K., Smith, R.C., Kim, H.S., 2000. Vascular cell apoptosis in remodeling, restenosis, and plaque rupture. Circ. Res. 87, 184–188.

Wang, S., Wu, Z., Sorenson, C.M., Lawler, J., Sheibani, N., 2003. Thrombosponin-1-deficient mice exhibit increased vascular density during retinal vascular development and are less sensitive to hyperoxia-mediated vessel obliteration. Dev. Dyn. 228, 630–642.

Xin, X., Yang, S., Ingle, G., Zlot, C., Rangell, L., Kowalski, J., Schwall, R., Ferrara, N., Gerritsen, M.E., 2001. Hepatocyte growth factor enhances vascular endothelial growth factor-induced angiogenesis in vitro and in vivo. Am. J. Pathol. 158, 1111–1120.

Zhang, Y., Stone, J., 1997. Role of astrocytes in the control of developing retinal vessels. Invest. Ophthalmol. Visual Sci. 38, 1653–1666.